work is PLANETSAVER®LED string light whose technical characteristics are presented in Table I.

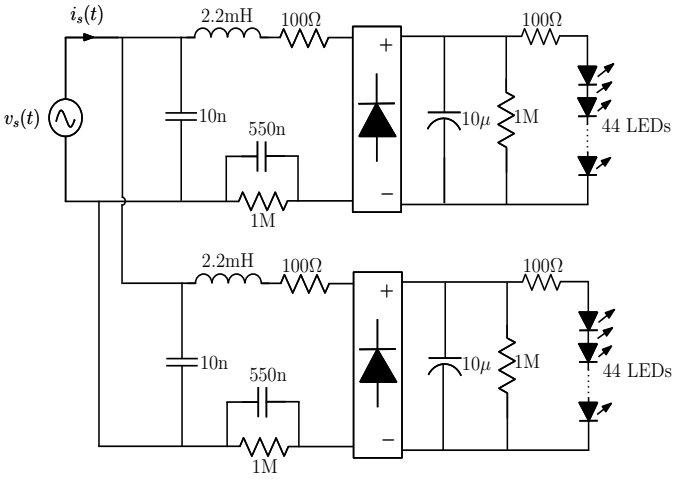

Fig. 1. Schematic circuit diagram of a commercial LEDs lamp.

TABLE I
CHARACTERISTICS AND PARAMETERS OF LEDS LAMP

Parameter	Value
Type	PLANETSAVER®LED string light
Lamp dimensions	20*44*820 mm
Supply Voltage	(110 - 220) V
Frequency f_l	(50 - 60) Hz
Current for 110 V	110 mA
Current for 220 V	52 mA
Power	12 W
Power Factor	0.55
Light Output	132 cd
Number of LEDS	88
Weight	280 g
Lamp life	10 years continuous operation

In spite of the LEDs lamps advantages, they are one of the main causes of harmonic distortion. Nonetheless, such distortion can be handled using a PFC controller. Although, a variety of power electronics circuit topologies and control methods can be used in PFC application [7], [8], the Continuous Conduction Mode (CCM) boost converter is commonly preferred for many applications. Namely, the existence of an inductor at the input of the boost converter is an advantage to use it in PFC providing a continuous (non pulsating) input current that can be controlled with current mode control techniques to force the input current to track the input line voltage. Broadly speaking, we can refer to PFC as a control which consists of a boost converter (BC) working under a hysteretic controller that is in charge of raising the voltage and adjust the power factor. A special characteristic of this converter with the control strategy for the current input loop based on a hysteresis band is it has variable switching frequency. Fig. 1 is the circuit diagram of a typical driver used in a commercial LEDs lamp.

The scheme used for the control design employed in this work is similar to that presented in [9]. Detailed design of the control will be presented in another paper written by one of the authors and for this reason it is not explained in this study. This work is only focused on the spectral signal analysis.

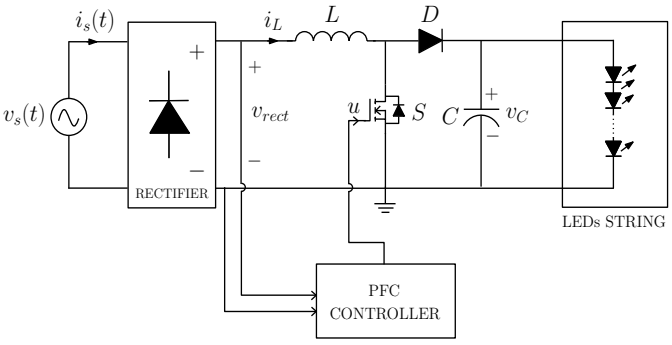

Fig. 2. Schematic diagram of a PFC boost converter working as LEDs lamp driver.

Figures 3 and 4 depict the simulated voltage and current drawn from the power supply regarding non-controlled (conventional commercial LED lamp) and controlled (adding PFC) circuit, respectively. Simulated signals are obtained by means of PSIM power package by setting the sampling frequency as 2 MHz, RMS voltage as 220 (thus the peak voltage is 311 V) and frequency $f_0 = 50$ Hz.

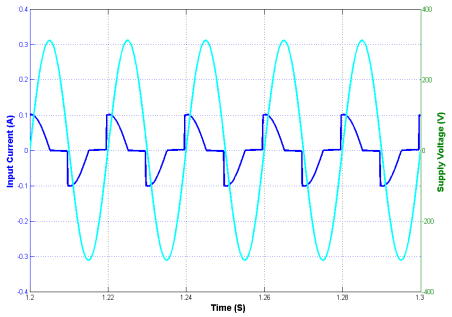

Fig. 3. Input line voltage and current of commercial LEDs lamp obtained from numerical simulation using PSIM package. PF≈ 0.55, THD$\approx \%151$

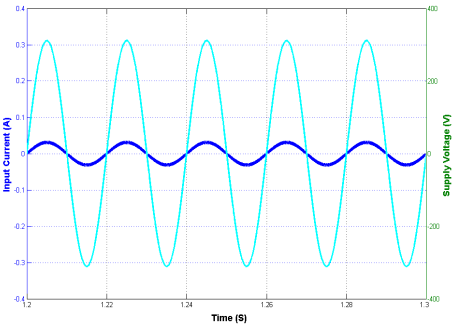

Fig. 4. Input line voltage and current of the designed system obtained from numerical simulation using PSIM package. PF≈ 0.99, THD$\approx \%10$

Throughout this paper, we refer to circuits from Fig. 1 as non-controlled circuit (NC). Similarly, circuit from Fig. 2 is named controlled circuit (CC). Thus, corresponding current signals are to be $i_{NC}(t)$ and $i_{CC}(t)$, respectively.

Figure 5 are the real experimental waveforms measured in both considered circuits with a RMS voltage value 220 V and a frequency of 50 Hz. Both of electrical signal are measured on the system input.

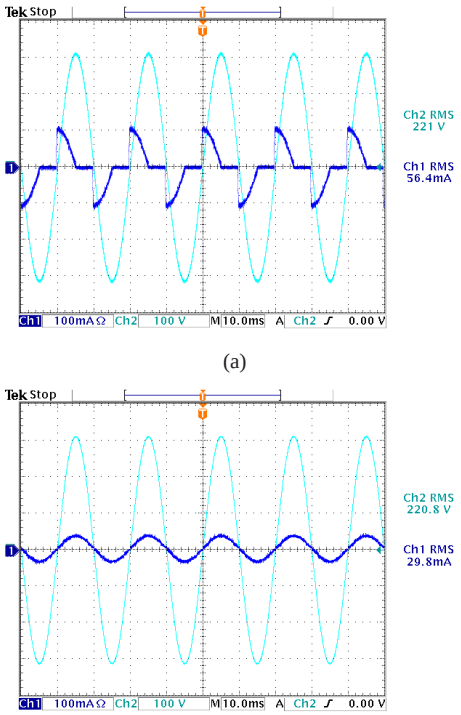

Fig. 5. LEDs lamp experimental waveforms. Channel 1: Input current; Channel 2: Input voltage (a) LEDs lamp without designed controller (PF≈ 0.55, THD≈ %151) (b) LEDs lamp with designed controller (PF≈ 0.98, THD≈ %10.9).

III. Spectral Analysis of Electrical Signals

Spectral analysis is done by two PSD estimations, namely, periodogram and discrete Fourier transform (DFT).

A. Discrete Fourier transform (DFT)

In power system analysis, Fourier transform (FT) is widely used and recommended to characterize electrical signals within the frequency domain [10]. This fact stems from the FT's simplicity and non-parametric nature.

Given a discrete signal $s = [s_0, \ldots, s_{N-1}]$ being N the signal length, the corresponding discrete Fourier transform (DFT) $S = [S_0, \ldots, S_{N-1}]$ can be calculated as follows:

$$S_k = \mathfrak{F}\{s\} = \sum_{n=0}^{N-1} s_n e^{-j\frac{2\pi nk}{N}} \tag{1}$$

for $k \in \{0, \ldots, N-1\}$.

Then, the Fourier-based PSD estimation P_{FT} is

$$P_{FT}(k) = |S_k| \tag{2}$$

where $|\cdot|$ is the modulus of the complex number.

B. Periodogram

This method is another approach to calculate the PSD of the discrete signal s using a periodogram [11]. PSD is calculated in units of power per radians per sample and the corresponding vector of frequencies is computed in radians per sample. Periodogram-based PSD P estimation for a determined frequency f is as follows:

$$P_{per}(f) = \frac{1}{N}\left|\sum_{n=1}^{N} s_n e^{-j2\pi f}\right|^2 \tag{3}$$

This PSD approach corresponds to the squared modulus of the discrete-time FT [12]. Discrete-time FT unlike DFT shown in (1) calculates the spectrum regarding a set of established frequencies given by f. DFT calculation is biased to k/N.

IV. Experimental Setup

The focus of this work lie in assessing the capability of periodogram to characterize the electrical signals for quantifying both the harmful effect of LEDs lamp non-controlled current and the quality of that obtained by the controlled circuit. To this end, two experiments are carried out. The first one is to determine the quality of the electrical current obtained after connecting PFC. In other words, this experiment is aimed to establish a way for properly quantifying the electrical current waveform resulting from controlled circuit. The second one consists of analyzing the spectrum to establish a numerical set of characteristics to quantify the quality of electrical current through the conventional LEDs lamps.

Periodogram is calculated in such a manner f is spanned over specific bandwidths set according to what interests to be analyzed. Likewise, after calculating DFT, in order to match the values of k to frequency values, vector $[0, \ldots, N-1]$ must be adjusted in terms of length and amplitude using the next power of 2 from length of signal and sampling frequency Fs.

For experiments, current signals as well as spectra are normalized to set the amplitude values ranged into the interval $[-1, 1]$. Then, if x is either a spectrum or a signal vector, the normalized vector $\hat{x}$ is:

$$\hat{x}_n = \frac{x_n}{\max|x|} \tag{4}$$

By applying this normalization the amplitude effect is discarded for further analysis.

Besides the measured signals, a reference (ideal) current signal $i = [i_0, \ldots, i_{N-1}]$ is taken into account, which is in the form:

$$i_n = \sin\left(2\pi n f_0 (Ts + 0.1s)\right), \tag{5}$$

where $Ts = 1/Fs$ is the sampling time, $Fs = 2MHz$, $f_0 = 50Hz$ and $n \in \{0, \ldots, N-1\}$. Reference signal has the same length and time interval $[0.1, 0.3]s$ as the original ones.

From the DFT of current signal, the total harmonic distortion THD can be calculated as follows:

$$THD = \sqrt{\frac{P_{FT}(f_0)^2}{\sum_{n=0}^{\infty} P_{FT}(nf_0)^2} - 1} \approx \sqrt{\frac{P_{FT}(f_0)^2}{\sum_{n=0}^{N_H} P_{FT}(nf_0)^2} - 1} \tag{6}$$

Indeed, $P_{FT}(nf_0) = \sqrt{a_n^2 + b_n^2}$ and the RMS value associated to n-th harmonic is $\sqrt{(a_n^2 + b_n^2)/2}$, where a_n and b_n are the Fourier series coefficients. THD can be approximated considering a finite number of harmonics N_H, in such a manner that the frequency $N_H f_0$ corresponds to 90 % of accumulated spectral power.

In other words, the area under the curve of P_{FT} within the interval $[0, N_H f_0]$ to be the 90 % of the area under the whole spectrum. Then, THD is estimated by using the harmonics that most contribute to the spectral information. A graphic explanation to set N_H is shown in Fig. 6.

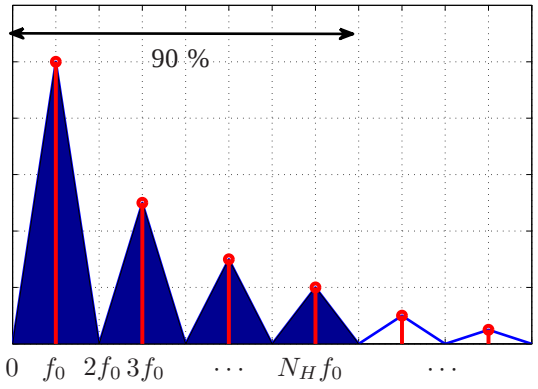

Fig. 6. Accumulated spectral power at 90 % regarding the number of harmonics

Likewise, we can estimate the distortion (δ) and displacement (DF) factor as:

$$\delta = \frac{1}{\sqrt{1 + THD_i}} \tag{7}$$

$$DF = \frac{PF}{\delta} \tag{8}$$

where PF is the nominal power factor. Also, the phase ϕ can be determined as

$$\phi = \cos^{-1}(DF) \tag{9}$$

V. Results and Discussion

A. Quality of electrical current after PFC

Fig. 7 shows the PSD-based FT spectra of input current signals for NC and CC circuit as well as the reference signal. The harmonic distortion is plainly seen in Fig. 7(b), where the power of third and fifth harmonic is approximately 40 % and 18 % of that associated to fundamental harmonic.

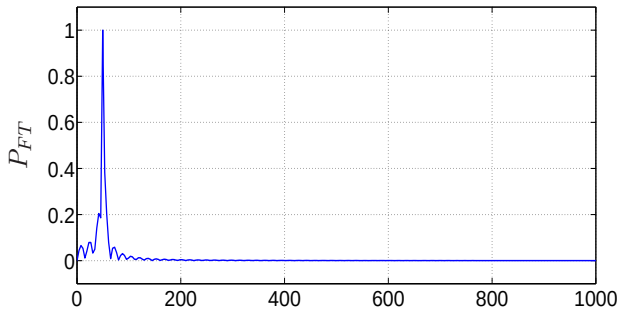

(a) Reference signal

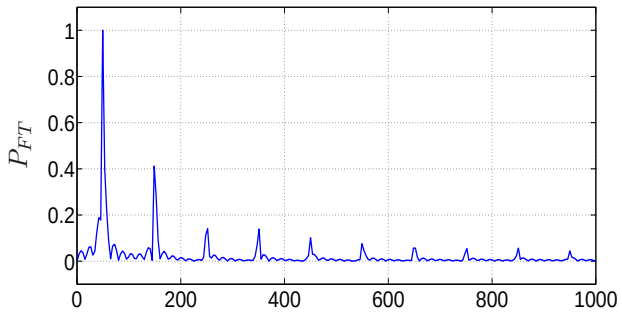

(b) Non-controlled circuit signal

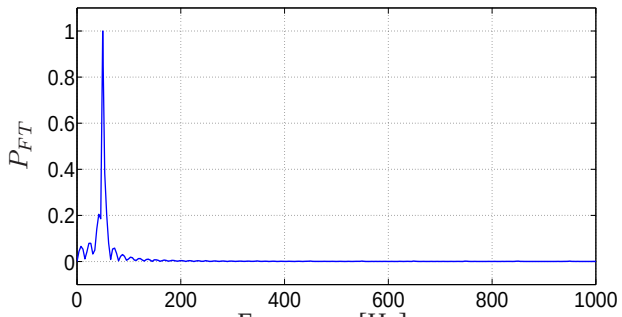

(c) Controlled circuit signal

Fig. 7. PSD-based FT for electrical current

In Fig. 8, the periodogram for NC, CC and reference signal are shown.

We can appreciate that from typical Fourier transform, being the most used in power system analysis, it can be inferred that the resultant electrical current from CC has approximately the same spectrum of that corresponding to

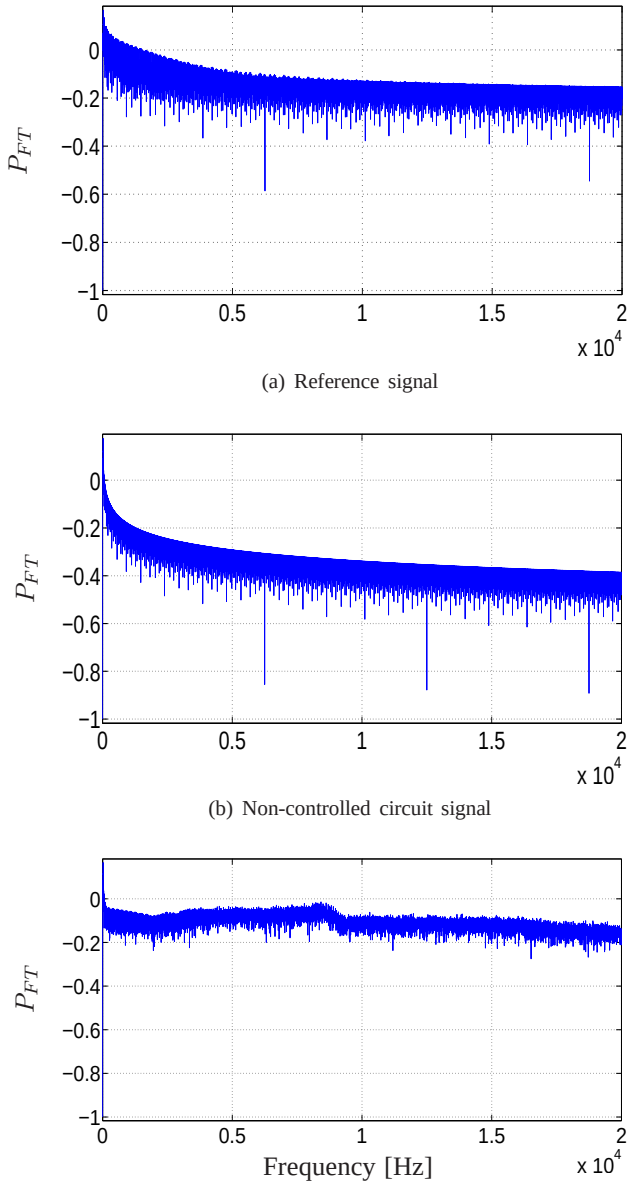

(a) Reference signal

(b) Non-controlled circuit signal

(c) Controlled circuit signal

Fig. 8. Periodogram for electrical current

the reference signal.

This fact can also be noticed by calculating the mean square error (MSE) between the spectrum of reference signal and that of $i_{CC}(t)$, as presented in Table II. Meanwhile, periodogram yields a more significant MSE between spectra. Therefore, periodogram is a suitable alternative to Fourier transform to estimate the PSD since it keeps more meaningful spectral information than conventional FT.

FT is able to detect the high frequency effect caused by the commutation frequency, which is given by the underlying hysteresis process and in range between 5 KHz and 20 KHZ, as seen in Fig. 9. It is important to highlight that spectral

TABLE II
MSE BETWEEN THE SPECTRA

MSE	FT	Periodogram
i vs i_{CC}	1.264×10^{-8}	0.0863
i vs i_{NC}	1.4792×10^{-6}	0.0718

power of high frequencies is very low, it is of order of 10^{-3}, and then it has not affectation over MSE calculation neither relevant spectral information in terms of envelope plotting. In contrast, periodogram exhibits significantly changes along the spectral power plotting which can be interpreted regarding specific frequencies and circuit conditions, and quantified by a measure characterizing the envelope shape, i.e. the area under curve.

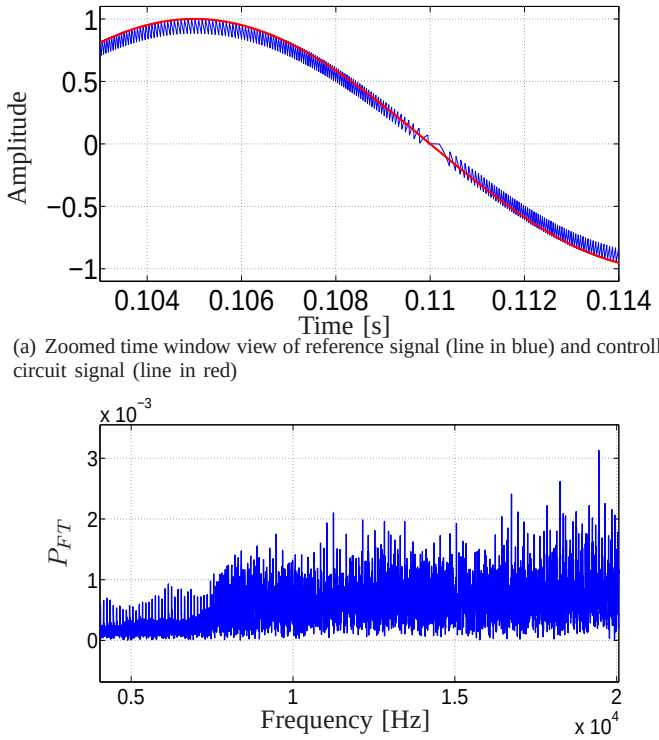

(a) Zoomed time window view of reference signal (line in blue) and controlled circuit signal (line in red)

(b) Fourier spectrum over high frequencies

Fig. 9. Hysteresis and high frequency effect

Also, it is noticeable that periodogram of CC signal (see Fig. 9) exhibits a rise in amplitude approximately in the range from 5 KHz and 10 KHz. This can be attributed to the commutation frequency.

B. Effect of electrical current in conventional LEDs lamps

As discussed in previous section, periodogram may be another alternative to analyze the electrical current on LEDS lamps. Now, we are focused on analyzing the PSD in lower frequencies (less than 1 KHz). In fig. 10, the periodogram of NC signal is shown. It is remarkable the periodical behavior evidenced over the envelope plotting. Experimentally, we

prove that a certain range of frequency has a similar shape along the periodogram plotting. Such range of frequency is here termed periodicity bandwidth (Δ_f). In order to test the behavior of Δ_f regarding the source frequency, we simulate a sweep on the value of f_0 in a range of frequencies close to 50 Hz, as it can be appreciated in Table III. The mean and standard deviation of Δ_f values estimated along 1 KHz corresponding a determined f_0 are arranged in the second column.

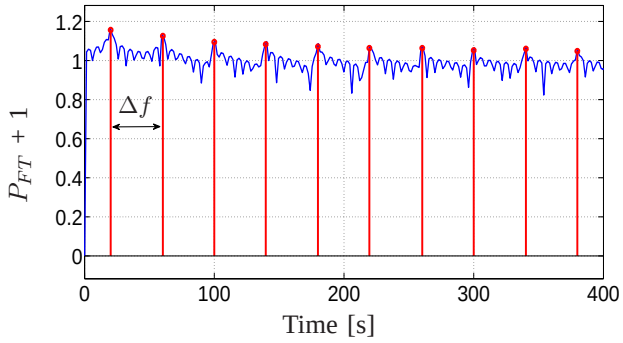

Fig. 10. Spectral periodicity factor

Also, from the periodicity frequency is possible to estimate the ratio between Δ_f and f_0, named spectral periodicity factor α, as:

$$\alpha = \frac{\Delta_f}{f_0} \tag{10}$$

In the third column from Table III, the mean and standard deviation of estimated values of α corresponding to each Δ_f are shown. We can notice that α is approximately a constant being its value 0.8. Then, we can infer that periodicity factor equating 0.8 may be considered as an additional meaningful characteristic of LEDs lamps.

TABLE III
SPECTRAL PERIODICITY RESULTS

f_0	Δ_f	Spectral periodicity factor α
30 Hz	24.007 $\pm$ 0.389	0.800 $\pm$ 0.013
40 Hz	32.006 $\pm$ 0.377	0.800 $\pm$ 0.009
50 Hz	39.999 $\pm$ 0.392	0.799 $\pm$ 0.0078
60 Hz	47.989 $\pm$ 0.395	0.799 $\pm$ 0.007
70 Hz	56.001 $\pm$ 0.385	0.800 $\pm$ 0.005
80 Hz	64.000 $\pm$ 0.405	0.800 $\pm$ 0.005

Then, as an outcome of this study, the set of characteristics summarized in Table IV is achieved. As noted, THD for i_{NC} is of 151.1 %, which means that the commercial LED lamp driver draw a pulsating input current producing a low power factor of 0.55 and consequently a high harmonic distortion. For signal i_{CC}, THD is of 11.3 % corresponding to a phase of 9.5169°. This value might be ideally 0°. Nevertheless, phase reached is still close to the ideal value. In addition, THD value obtained by the estimation proposed here is approximated to that calculated over the implemented circuit that is 151.1 % (see Fig. 1).

TABLE IV
SET OF SPECTRAL CHARACTERISTICS FOR LEDS LAMPS

Signal	THD %	PF	δ	DF	ϕ	α
i_{NC}	151.1	0.55	0.5519	0.9966	4.7495°	0.8
i_{CC}	11.3	0.98	0.9937	0.9862	9.5169°	N/A

VI. CONCLUSIONS AND FUTURE WORK

In this paper, a commercial LED lamp driver that draw a pulsating input current y un high efficiency LED driver based PFC circuit has been analized. This work proves that other frequency-based representation approaches can provide substantial spectral information that can be hidden when using conventional Fourier transform. In particular, periodogram is considered. This power spectral estimation exhibits more changes along its plotting when analyzing the circuit without applying PFC in both high and relatively low frequencies. Then, it provides more meaningful spectral information. In fact, in high frequency permit us to determine the effect of commutation frequency. Also, as a remarkable result of this work is to mention that a set of LEDs lamps characteristics is introduced, including a novel periodicity factor.

For further works, we are interested in analyzing in detail the spectra to relate spectral power to real circuit conditions.

ACKNOWLEDGEMENTS

Authors would like to thank Universidad Cooperativa de Colombia - Pasto, Department of Electronics Universidad de Nariño and Departament d'Enginyeria Electrònica, Elèctrica i Automàtica, Escola Tècnica Superior d'Enginyeria, Universitat Rovira i Virgili, 43007, Tarragona, Spain.

REFERENCES

[1] H.-J. Chiu, Y.-K. Lo, J.-T. Chen, S.-J. Cheng, C.-Y. Lin, and S.-C. Mou, "A High-Efficiency Dimmable LED Driver for Low-Power Lighting Applications," *Industrial Electronics, IEEE Transactions on*, vol. 57, no. 2, pp. 735 –743, feb. 2010.

[2] C.-Y. Wu, T.-F. Wu, J.-R. Tsai, Y.-M. Chen, and C.-C. Chen, "Multistring LED Backlight Driving System for LCD Panels With Color Sequential Display and Area Control," *Industrial Electronics, IEEE Transactions on*, vol. 55, no. 10, pp. 3791 –3800, oct. 2008.

[3] S. Hui, S. Li, X. Tao, W. Chen, and W. Ng, "A novel passive offline light-emitting diode (led) driver with long lifetime," in *Applied Power Electronics Conference and Exposition (APEC), 2010 Twenty-Fifth Annual IEEE*, feb. 2010, pp. 594 –600.

[4] J. Alonso, J. Vina, D. Vaquero, G. Martinez, and R. Osorio, "Analysis and Design of the Integrated Double Buck-Boost Converter as a High-Power-Factor Driver for Power-LED Lamps," *Industrial Electronics, IEEE Transactions on*, vol. 59, no. 4, pp. 1689 –1697, april 2012.

[5] J. Cardesin, J. Ribas, J. Garcia-Garcia, M. Rico-Secades, A. Calleja, E. Corominas, and M. Dalla Costa, "LED Permanent Emergency Lighting System Based on a Single Magnetic Component," *Power Electronics, IEEE Transactions on*, vol. 24, no. 5, pp. 1409 –1416, may 2009.

[6] H.-J. Chiu and S.-J. Cheng, "LED Backlight Driving System for Large-Scale LCD Panels," *Industrial Electronics, IEEE Transactions on*, vol. 54, no. 5, pp. 2751 –2760, oct. 2007.

[7] A. El Aroudi and M. Orabi, "Stabilizing Technique for AC-DC Boost PFC Converter Based on Time Delay Feedback," *IEEE Trans. Circuits and Systems II: Express Briefs*, vol. 57, no. 1, pp. 56–60, Jan. 2010.

[8] B. Singh, B. Singh, A. Chandra, K. Al-Haddad, A. Pandey, and D. Kothari, "A review of single-phase improved power quality AC-DC converters," *IEEE Trans. Industrial Electronics*, vol. 50, no. 5, pp. 962–981, Oct. 2003.
[9] X. M. J. Zou and C. Du, "Asymmetrical oscillations in digitally controlled power-factor-correction boost converters," *Circuits and Systems II: Express Briefs, IEEE Transactions on*, vol. 56, 2009.
[10] T. Okamoto, S. Kawata, and S. Minami, "Fourier transform spectrometer with a self-scanning photodiode array," *Applied optics*, vol. 23, no. 2, pp. 269–273, 1984.
[11] P. Welch, "The use of fast fourier transform for the estimation of power spectra: a method based on time averaging over short, modified periodograms," *Audio and Electroacoustics, IEEE Transactions on*, vol. 15, no. 2, pp. 70–73, 1967.
[12] A. V. Oppenheim, R. W. Schafer, J. R. Buck *et al.*, *Discrete-time signal processing*. Prentice Hall Upper Saddle River, 1999, vol. 5.